

HEAT AND MASS TRANSPORT AT UNSTEADY SUBLIMATION OF SINGLE METAL-ORGANIC PARTICLES IN THE GAS-CARRIER FLOW

Abdrakhmanov R.Kh.¹, Igumenov I.K.^{2*}, Lukashov V.V.^{1,2}, Makarov M.S.¹, Makarova S.N.^{1,2}

*Author for correspondence

¹ Kutateladze Institute of Thermophysics Siberian Branch of RAS
630090 Novosibirsk, 1 Lavrentiev ave.

² Nikolaev Institute of Inorganic Chemistry, Siberian Branch of RAS
630090 Novosibirsk, 3 Lavrentiev ave.

E-mail: igumen@niic.nsc.ru

ABSTRACT

The results of experimental research and numerical modeling of convective heat and mass transfer during the sublimation of spherical particles of beta-diketonates of metals Cr(acac)₃ and Zr(dpm)₄ in a high-temperature flow of an inert gas (argon or helium) are presented. The sublimation process is visualized. The temperature and particle size dynamics are obtained. The effect of the carrier-gas properties on the sublimation intensity of the particles with different initial diameters in the temperature range from 200 to 330 °C is analyzed. It is shown that under the conditions of a high intensity of substance removal from the phase transition surface, the time for complete sublimation of the sample of Cr(acac)₃ and Zr(dpm)₄ may be less than the time, required to establish an equilibrium temperature between the precursor particle and the vapor-gas flow.

INTRODUCTION

A shift towards the modular integration of power thermal parameters of the precursor are significant limitations of sublimation rate in the processes of functional coatings using beta-diketonates of metals during chemical vapour deposition (MO CVD). The low pressure of saturated vapour at operating temperature of sublimation process and low thermal stability of compounds do not allow high concentration of precursor vapours in the deposition zone sufficient to produce the coatings of desired thickness at a high rate. Therefore, an actual task for the formation of effective precursor vapour sources is an increase in intensity of sublimation due to intensification of radiative- convective heat exchange on the surface of precursor particles in the carrier gas flow.

In the literature, there are a limited number of papers devoted to the study of heat and mass transfer during sublimation. One can note the study of transport processes during sublimation of ice [1] at cryogenic temperatures. Mass transfer in the sublimation process of metal-organic compounds was considered in [2-4]. The generalizing mass and heat transfer correlation dependencies were received. The experimental conditions in these studies allowed accepting the assumption that the temperatures of the argon-filled reactor and the phase transition surface were equal. Such statement may be incorrect for high-intensity sublimation of particles, suspended in the carrier gas stream. An important feature of high-intensity

NOMENCLATURE

Δh	[J/kg]	Specific enthalpy of sublimation
C	[W/m ² /K ⁴]	Stefan–Boltzmann constant
c_p	[J/kg/K]	Specific heat capacity
D	[m ² /s]	Diffusivity coefficient of binary mixture
d	[m]	Diameter of particle
j	[kg/m ² /s]	Mass flux of gas mixture
K	[-]	Mass fraction of species in mixture
m	[kg]	Mass of particle
Nu	[-]	Thermal Nusselt number
p	[Pa]	Pressure
Pr	[-]	Prandtl number
R	[m]	Radius of particle
r	[m]	Radial coordinate
Re	[-]	Reynolds number
Sc	[-]	Schmidt number
Sh	[-]	Sherwood number
Le	[-]	Lewis number
T	[K]	Absolute temperature
t	[°C]	Temperature
u	[m/s]	Velocity of inert gas flow

Special characters

ϵ_{ef}	[-]	Effective emissivity
λ	[W/m/K]	Thermal conductivity coefficient
ρ	[kg/m ³]	Density
τ	[s]	Time

Subscripts and superscripts

c	Center of particle
cr	Crystal
e	External flow
g	Gas phase
p	Pressed particle
s	Solid phase
w	Gas-solid interface
0	Initial conditions
1	Precursor
2	Inert gas (Ar or He)

sublimation in the gas flow is reduction of convective heat transfer to the phase transition surface due to intense transverse vapor flux, injected from the particle, which was not taken into account in the above mentioned studies.

Various thermodynamic states of matter: stable, metastable and labile are analyzed in [5] in the description of sublimation. It is noted, in particular, that in the case of crystallinity sublimation, large grains sublimate more slowly than smaller structural formations.

If the steam becomes supersaturated, embryo formation and desublimation occur. The important factor on which the

desublimation depends is the ratio of heat and mass transfer intensities (i.e. whether the growth of the solid phase occurs on the substrate surface or in the gas phase) [6]. The direction of the process can be estimated by analyzing the value of the Lewis number Le . If $Le > 1$ the heat exchange occurs more intensively than mass transfer, and the transition to the solid phase occurs not on the surface of the particle (reactor wall) but in the flow. Some peculiarities of heat and mass transfer in the phase transition arising in binary systems with $Le \neq 1$ are considered in [7-9].

In the paper we present the results of experimental studies and numerical simulations of the kinetics of sublimation of a single spherical precursor particle in an inert gas stream.

EXPERIMENTAL PROCEDURE

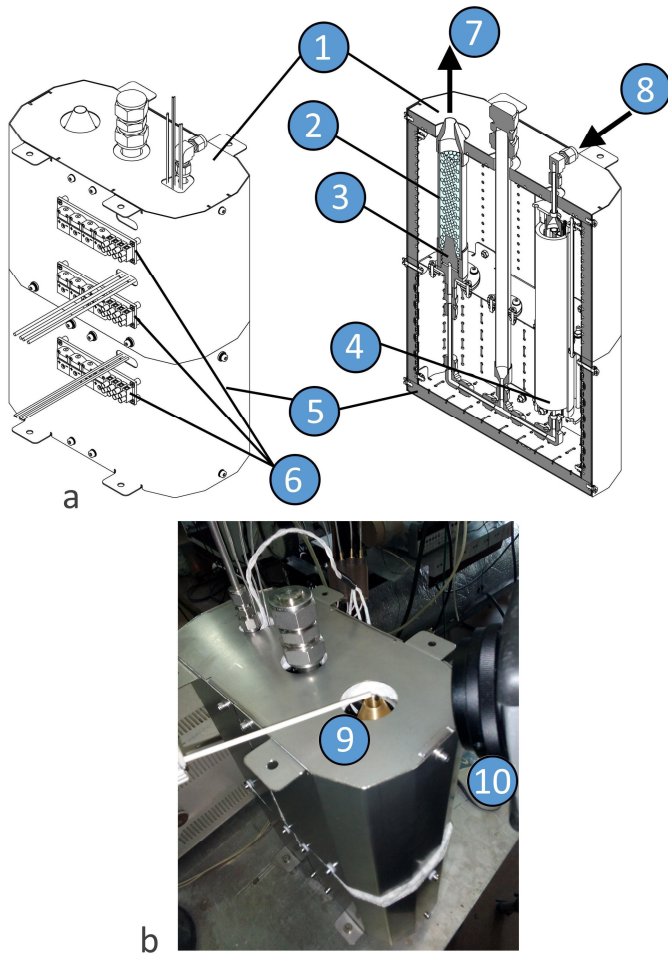


Figure 1 The scheme (a) and the photograph (b) of the device for the flow preparation: 1 – upper part of the thermostat, 2 – nozzle apparatus filled with quartz beads, 3 – gas distributor, 4 – tubular heater, 5 – lower part of the thermostat, 6 – electrical commutation unit, 7 – supply of inert gas, 8 – outlet of heated gas, 9 – test sample, 10 – video camera (thermal imager).

To study the heat and mass transfer during sublimation a number of samples were prepared from precursor with

characteristic crystal size of $\text{Cr}(\text{acac})_3$ and $\text{Zr}(\text{dpm})_4$ of about 20-50 μm . The source material was wetted with heptane and pressed to obtain a spherical bead using metallic mold. Samples were spheres with diameters of 4 mm with micro-thermocouples of type K. Diameter of thermo-electrodes was 100 μm . A sample with an initial room temperature was placed in a heated stream of argon or helium at atmospheric pressure. The flow preparation device is shown on Figure 1. An axisymmetric jet of gas with velocity and temperature constant along the radial nozzle flowed onto the studied sample from the profiled nozzle. The gas stream preparation system was placed inside a thermostated housing, equipped with PID control systems. The flow temperature was set in the range from 200 to 330 $^{\circ}\text{C}$. Measurements of convective and radiant heat fluxes at a distance of one nozzle diameter (12 mm), made with the help of a gradient heat flow sensor, showed that the contribution of radiation to the total heat flux at the surface without sublimation did not exceed 20%. The gas supply in our experiments was carried out by the digital flow controllers and was set at 8 slm.

NUMERICAL METHOD

Numerical simulation was based on the physico-mathematical model of non-stationary sublimation of a single particle of the spherical precursor that flows in the gas stream of a medium-pressure carrier gas flow. The sublimation process was assumed to occur uniformly from the entire surface of the solid particle; a volumetric sublimation inside the pores of the material was not taken into account; and the particle of the precursor did not lose spherical symmetry over time.

At low flow velocities (diffusion sublimation regime), the heat and mass transfer processes in the gas phase are described by a system of parabolic second-order differential equations in partial derivatives of heat conductivity and diffusion [10]:

$$c_p^g \rho^g \frac{\partial T}{\partial \tau} = \frac{1}{r^2} \frac{\partial}{\partial r} \left(r^2 \lambda^g \frac{\partial T}{\partial r} \right) + \rho^g D (c_{p1}^g - c_{p2}^g) \frac{\partial T}{\partial r} \frac{\partial K_1^g}{\partial r}; \quad (1)$$

$$\rho^g \frac{\partial K_1^g}{\partial \tau} = \frac{1}{r^2} \frac{\partial}{\partial r} \left(\rho^g D r^2 \frac{\partial K_1^g}{\partial r} \right), \quad K_2^g = 1 - K_1^g. \quad (2)$$

At high flow velocities (convective sublimation regime), the Rantze-Marshall similarity relations determine the heat and mass transfer on the particle surface:

$$\text{Nu} = 2 + 0.6 \text{Re}_d^{0.5} \text{Pr}^{1/3}, \quad \text{Sh} = 2 + 0.6 \text{Re}_d^{0.5} \text{Sc}^{1/3}. \quad (3)$$

The temperature of a solid particle, regardless of the sublimation regime, is described by the heat conduction equation of the form:

$$c_p^s \rho^s \frac{\partial T}{\partial \tau} = \frac{1}{r^2} \frac{\partial}{\partial r} \left(r^2 \lambda^s \frac{\partial T}{\partial r} \right). \quad (4)$$

The system of equations (1-4) was supplemented with the state equation of ideal gas for the mixture of precursor vapor and gas carrier, data on thermodynamic and transport properties of the precursor in the solid and vapor states, value of sublimation enthalpy, and temperature dependence of precursor vapor pressure [11-15].

At the initial time the radius R_w and the temperature of the precursor particle t_0^s are given. In the diffusion sublimation

regime the size of the region occupied by the gas phase R_e was set for $R_e \gg R_w$. In the gas phase region the temperature at the initial time was T_0^g and the concentration of precursor vapor $(K_1^g)_0$ was zero. The pressure p_e was kept constant. In the convective mode of sublimation the gas phase region was not modeled. The thermal and diffusion fluxes at the interfacial surface are determined by the heat and mass transfer laws depending on the Reynolds number (3). The Reynolds number was determined from the diameter of the precursor particle and the relative velocity of flow around the particle by a stream of argon or helium u_e .

Boundary conditions at $r=0$ were: $\partial T/\partial r=0$, $\partial K_1^g/\partial r=0$ at $r=R_e$ (in diffusion mode), $\partial T/\partial r=0$, $\partial K_1^g/\partial r=0$. The temperature at the interfacial surface was determined from the heat balance:

$$\left(\lambda^g \frac{\partial T}{\partial r}\right)_{R_w^+} + \left(\frac{\rho^g D}{1-K_1^g} \frac{\partial K_1^g}{\partial r}\right)_{R_w^+} \Delta h + \varepsilon_{ef} C(T_w^4 - T_e^4) = \left(\lambda^s \frac{\partial T}{\partial r}\right)_{R_w^-}.$$

In the convective mode of sublimation:

At $r=R_w^-$ $\partial K_1^g/\partial r=0$. The precursor vapor mass fraction $(K_1^g)_w$ at the interfacial surface $r=R_w^+$ is related to the temperature of the sublimating surface T_w by the equation of the vapor saturation curve of the corresponding precursor. The position of the interface is determined from the solution of equation:

$$\frac{\partial R_w}{\partial \tau} = \frac{1}{\rho_{R_w^s}^s} \left(\frac{\rho^g D}{1-K_1^g} \frac{\partial K_1^g}{\partial r} \right)_{R_w^+}. \quad (5)$$

The main feature of the solution method is the integration of the outlined system of differential equations in moving coordinates: $\xi^g = \xi^s = \tau$ (time) and $\eta^g = (r-R_w)/(R_e-R_w)$, $\eta^s = r/R_w$, (respective radial coordinates for the gas-vapor mixture and the solid particle region). The position of the phase transition boundary is determined from the intensity of sublimation and depends on the time (5). The computational grid in physical coordinates is reconstructed at each step of integration over time. The explicit border allocation allows minimizing the computing time and improving the accuracy of the obtained results. The system of equations in new coordinates is discretized by an implicit scheme, and the resulting system of algebraic equations is solved by the sweep method. The nonlinearity of the system of equations is eliminated by the method of simple iterations at each step of integration over time.

DISCUSSION OF RESULTS

Figure 2 shows the top-down sequences of frames from video, obtained by visualizing the process of sublimation of precursors $\text{Cr}(\text{acac})_3$ and $\text{Zr}(\text{dpm})_4$ into the flow of Ar or He. The speed of the incoming argon flow was 1.9 m/s, and the one of helium was 2.1 m/s. During $\text{Cr}(\text{acac})_3$ sublimation the temperature of the oncoming stream was maintained equal to

210 ± 2 °C, and for the $\text{Zr}(\text{dpm})_4$ sublimation it was 250 ± 2 °C. It can be noted that the molded particles are somewhat flattened as the substance is carried away, but they do not lose symmetry with respect to the vertical axis, which gives grounds for applying the simplified model in numerical analysis. The thermograms of sublimation of a molded particle and a crystal of the same initial mass practically do not differ from each other. The experimental estimates show that the crystalline density of precursors is approximately twice as large as the density of the molded particle. With the same mass, the nominal diameter of the crystal $d^{cr} = d^p / \sqrt[3]{2} = 0.8d^p$ is only 20% less than the diameter of the molded particle. On the one hand, this can explain the weak effect of density on heat and mass transfer processes on the surface of particles; on the other hand, this gives grounds to extend the results of this study to the case of sublimation of single crystals in a carrier flow of an inert gas, which is characteristic of high-performance sublimators.

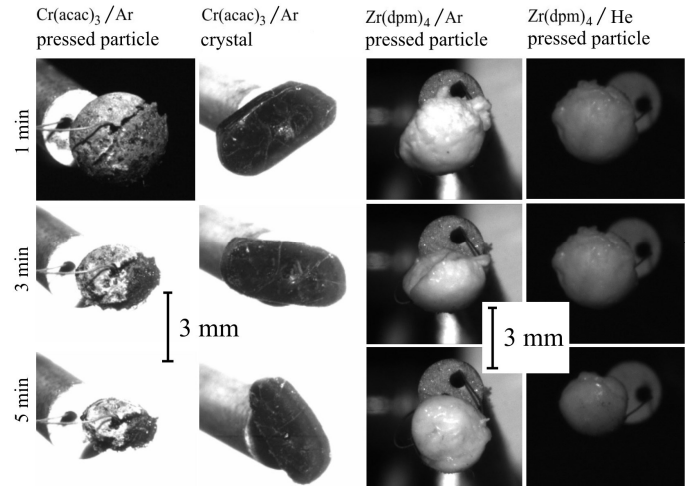


Figure 2 Visualization of precursors $\text{Cr}(\text{acac})_3$ and $\text{Zr}(\text{dpm})_4$ sublimation process into the Ar or He flow.

The right-hand side of Figure 2 shows the dynamics of the particle size variation $\text{Zr}(\text{dpm})_4$ upon sublimation into argon and helium. It is clearly seen that sublimation into the helium flow is much more intense than in the flow of argon. Figure 3 shows a thermogram of the $\text{Cr}(\text{acac})_3$ particle sublimation into argon, corresponding to the left-hand row of photographs in Figure 2. The data are presented in comparison with the results of numerical simulation. The temperature change process can be divided into three stages. The first stage is the particle heating from the initial room temperature to the equilibrium sublimation temperature for about 40 s. The second stage is temperature stabilization for about 580 s (with a weak growth in the experiment). The third stage is a sharp increase in temperature at the end of the sublimation process for about 20 s. As you can see from data presented at Figure 4, the results of numerical simulation are in good agreement with the experiment. It should be noted that to describe the level of equilibrium temperature and its growth in the third stage of the process one should take into account the radiation in the heat

transfer model. Although the contribution of radiation to the thermal balance at the phase transition boundary is not large (about 20%), the decrease in the equilibrium temperature of the particle leads to a significant decrease in the saturation pressure of the precursor vapor and consequently to a decrease in the sublimation intensity. Calculations show that the total sublimation time, obtained without taking radiation into account, is approximately half of the time of sublimation, obtained considering radiation. The reason of some temperature increase in the second stage of the process may be associated with the formation of large pores in the particle structure and with periodic contact of the hot stream and the junction of the thermocouple. This is especially noticeable at the end of the sublimation process, when the particle is a bundle of interwoven crystalline filaments, enveloping the thermocouple junction (see photo on the right in Figure 3).

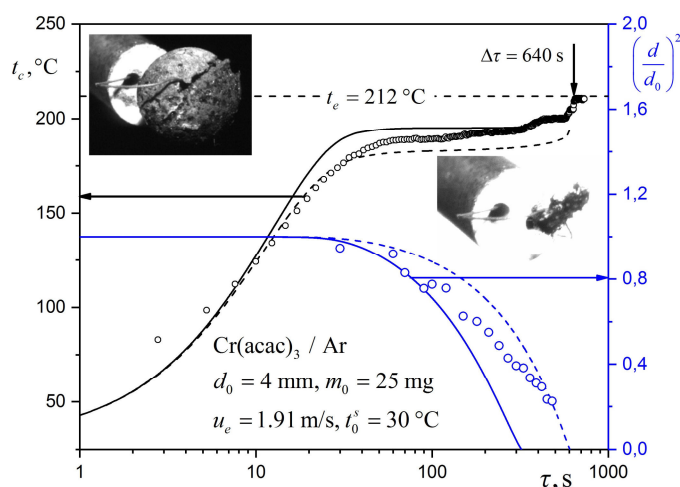


Figure 3 The temperature (scale on the left) and the diameter of the sample (scale on the right) of $\text{Cr}(\text{acac})_3$ change in time upon sublimation into the Ar flow: Solid lines – calculation without radiation; Dotted lines – taking into account radiation; Points – experimental data.

Figure 4 presents data on the sublimation of $\text{Zr}(\text{dpm})_4$ into an argon stream with a temperature of 287°C . It is seen that at the stabilization stage the temperature increase is substantially greater than for the precursor $\text{Cr}(\text{acac})_3$. Apparently, this is due to high influence of radiation, because the equilibrium temperature of the particle of $\text{Zr}(\text{dpm})_4$ in this experiment is much higher than in the experiment with $\text{Cr}(\text{acac})_3$. In particular, this is confirmed by the calculation results, presented in Figure 4 by solid lines, which are obtained taking into account radiant heat exchange with the environment. It can be noted that for this substance there are not enough reliable data on key thermodynamic and transport properties, especially for the vapor phase. The data presented in the literature even on saturation pressure diverge a few times, which significantly affects the intensity of sublimation obtained by calculation.

With a temperature drop of the incident flow upon sublimation of $\text{Zr}(\text{dpm})_4$ the temperature drift associated with the radiation is significantly reduced. At the stabilization stage,

the temperature of the studying sample ceases to change. Under certain conditions, the stabilization stage may disappear at all, and a stationary sublimation process may become impossible. All the time until the complete transition into the vapor phase, the temperature of the sample continuously changes.

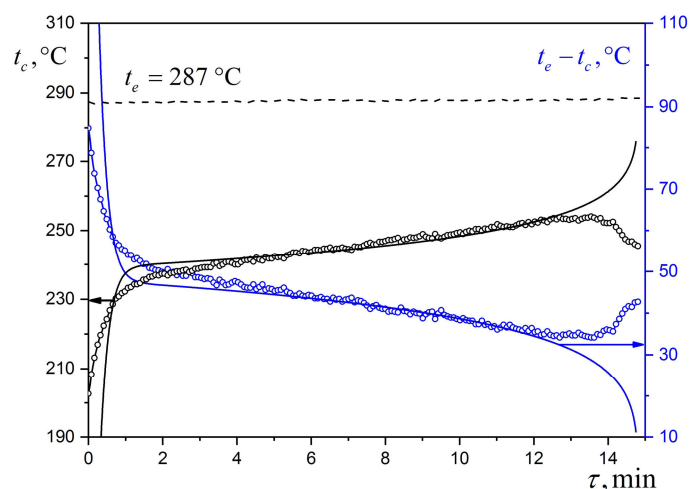


Figure 4 Changes of temperature of $\text{Zr}(\text{dpm})_4$ sample with a diameter of 4.5 mm at Ar flowing with velocity $u_e=1.91$ m/s.

The photo in the field of Figure 5 shows that when a $\text{Zr}(\text{dpm})_4$ particle is in the helium flow with a temperature of 277°C , the growth of thin dendroid crystals on the surface of the sample takes place. This process was not taken into account in numerical modeling, which can also be the reason for the discrepancy between the calculated data and the data of the $\text{Zr}(\text{dpm})_4$ sublimation experiment. It may be assumed that in the experiment due to the radiation heat loss from the stern part of the particle into the surrounding cold space the surface temperature is locally reduced. This may lead to partial desublimation of the precursor vapor. In the study of water ice sublimation into vacuum [16] the appearance of similar dendroid-like crystals was detected. The authors of [16] associated desublimation with manifestation of the phase transition non-equilibrium (local supersaturation of vapors).

It is interesting to note that regardless of reaching the stationary heat state of the particle, the time dependence of the relative diameter of the sample $(d/d_0)^2$ was close to the linear one (see Figure 5). It is known that for liquid drops a practically linear decrease in the square of the relative diameter corresponds to the diffusion mode of evaporation, when radiation and convection may be neglected. Such a mode of evaporation (sublimation) is characterized by a non-stationary of mass flux at the surface unlike the data of [2] where it was noted that when the beta-diketonates are sublimated from a flat wall the mass flux was constant during the stabilization stage.

The numerical simulation results obtained in this paper for the experimental conditions show a linear decrease in the square of the relative particle diameter versus time, and correlate well with the results of the sublimation experiment into the helium flux. As can be seen from Figure 5, sublimation of $\text{Zr}(\text{dpm})_4$ into helium occurs much more intensely than in the argon flow.

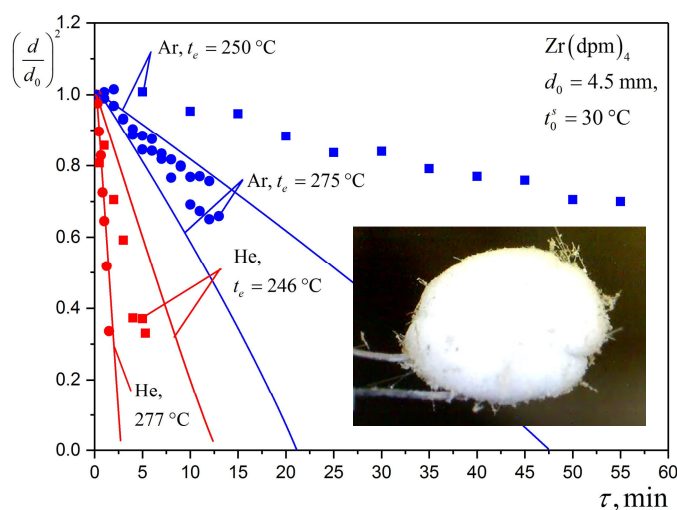


Figure 5 Change of the relative diameter of $Zr(dpm)_4$ sample in time during sublimation in a flow of argon or helium.

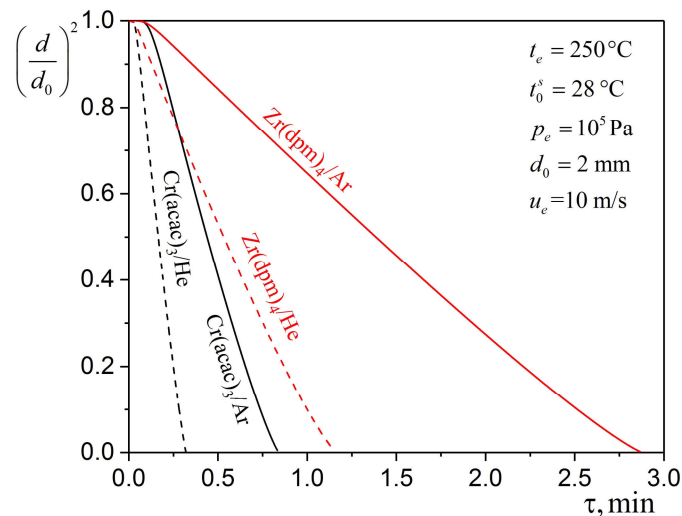


Figure 6 Changes in diameters of particles of chromium and zirconium β -diketonates depending on time of sublimation into various gases.

Figure 6 presents numerical modeling data, showing changes in relative particle diameter of chromium and zirconium β -diketonates in time during the sublimation to the carrier flow of argon and helium at a flow velocity of 10 m/s. The initial particle diameter was 2 mm. At an ambient flow velocity of 10 m/s the effect of convection is substantially increased. A smaller particle warms up more quickly however the high temperature at the end of the heating stage leads to an increase in the intensity of sublimation. The stationary thermal regime does not have time to establish itself in the time necessary for complete sublimation of the precursor particle under investigation. As can be seen from the graph with this sublimation mode the change in the square of the relative diameter ceases to obey the linear law. Comparison of the data on sublimation in argon and helium at high velocity of the flow around the particle shows that sublimation into helium is more intense in this case as well.

The increase in sublimation intensity is believed to be due to the fact that thermal conductivity and heat capacity of helium are higher than in argon. An increase in these parameters leads to an intensification of heat transfer at the boundary of the phase transition, which leads to an increase in the temperature of the particle and an increase in the vapor pressure at its surface. In addition, when sublimation occurs into the helium flow, the temperature difference between the incoming gas and the equilibrium temperature of the particle decreases during the stabilization stage. This may be important for CVD processes in which thermally unstable organometallic compounds are used. As you can see, helium is the best carrier gas for building high-performance flow-through sublimators.

CONCLUSION

The results of the study of radiation-convective heat and mass transfer during sublimation of spherical particles of $Cr(acac)_3$ and $Zr(dpm)_4$ beta metal diketonates into a high-temperature inert gas flow are presented. It is shown that heat exchange by radiation can lead to a substantial decrease in the saturation pressure of the precursor vapor and, consequently, to a decrease in the intensity of sublimation. The total sublimation time, obtained without taking radiation into account in numerical simulation is approximately half the time of sublimation obtained considering radiation.

Simultaneously with $Zr(dpm)_4$ sublimation, probably due to heat radiation from the stern part of the particle to the surrounding space, the surface temperature locally decreases, which leads to a partial desublimation of the precursor vapor. The growth of dendroid-like *crystals* was observed in the flow of a particle of $Zr(dpm)_4$ by a helium stream with a temperature of 277 °C. The results of numerical simulation showed that for fine particles, under conditions of intense convective heat and mass transfer, the time for complete sublimation is the same or shorter than the time for heating the particle to equilibrium temperature. Such a regime is characterized by higher intensity of the mass flow of matter from the particle surface compared to the equilibrium sublimation regime. Based on experimental data and simulation results, it has been shown that the use of helium as a carrier gas allows reducing the temperature difference between the flow and the precursor particle while maintaining high sublimation intensity, which may be important for CVD processes, where organometallic compounds may be thermally unstable.

ACKNOWLEDGMENTS

This work was supported by the Russian Science Foundation (grant No. 16-19-10325).

REFERENCES

- [1] Kucherov A.N., Sublimation and vaporization of an ice aerosol particle in the form of thin cylinder by laser radiation, *International Journal of Heat and Mass Transfer*, Vol. 43, 2000, pp. 2793-2806.
- [2] Fedotova N.E., Gelfond N.V., Igumenov I.K., Mikheev A.N., Morozova N.B., and Tuffias R.H., Experiment and modeling of mass-transfer processes of volatile metal beta-diketonates. I. Study of mass-transfer process of tris-(acetylacetonato) Chromium(III) at atmospheric pressure, *International Journal of Thermal Sciences*, Vol. 40, 2001, pp. 469-477.

- [3] Gelfond N.V., Mikheev A.N., Morozova N.B., Gelfond N.E., and Igumenov I.K., Experiment and modeling of mass-transfer processes of volatile metal beta-diketonates. II. Study of mass-transfer process of tris-(acetylacetonato) iridium(III), *International Journal of Thermal Sciences*, Vol. 42, 2003, pp. 725-730.
- [4] Cherepanov A.N., Shapeev V.P., Semin L.G., Cherepanova V.K., Igumenov I.K., Mikheev A.N., Gelfond, N.V., and Morozova N.B., Quasi-one-dimensional model of heat and mass transfer during sublimation of a molecular crystal plate in a plane channel, *Journal of Applied Mechanics and Technical Physics*, Vol. 44, Issue 4, 2003, pp. 543-548.
- [5] Savage J.R., Blair D.W., Levine A.J., Guyer R.A., and Dinsmore A.D., Imaging the sublimation dynamics of colloidal crystallites, *Science*, Vol. 314, No. 5800, 2006, pp. 795-798.
- [6] Smolkin P.A., Buynovskiy A.S., Lazarchuk V.V., Matveev A.A., and Sofronov V.L., Mathematical model of desublimation process of volatile metal fluorides, *Bulletin of the Tomsk Polytechnic University*, Vol. 310, No 3, 2007, pp. 69-71.
- [7] Lukashov V.V., On the determination of the surface temperature of an evaporating liquid, *Theoretical Foundations of Chemical Engineering*, Vol. 37, Issue 4, 2003, pp. 325-329.
- [8] Makarova S.N., and Shibaev A.A., Heat and mass transfer with evaporation cooling of a porous plate, *Journal of Physics: Conference Series*, Vol. 754, 2016, pp. 1-6.
- [9] Makarov M.S., and Makarova S.N., Heat and mass transfer at adiabatic evaporation of binary zeotropic solutions, *Thermophysics and Aeromechanics*, Vol. 23, No. 1, 2016, pp. 23-32.
- [10] Ranz M.E., and Marshall W.R., Evaporation from drops: Part I, *Chemical Engineering Progress*, Vol. 48, No. 3, 1952, pp. 141-146
- [11] Fox E.C., and Thomson W.J., Coupled heat and mass transport in unsteady sublimation drying, *American Institute of Chemical Engineers Journal*, Vol. 18, No. 4, 1972, pp. 792-797.
- [12] Semyannikov P.P., Igumenov I.K., Trubin S.V., Chusova T.P., and Semenova Z.I., Thermodynamics of chromium acetylacetonate sublimation, *Thermochimica Acta*, Vol. 432, 2005, pp. 91-98.
- [13] Morozova N.B., Sysoev S.V., Igumenov I.K., and Golubenko A.N., Study of temperature dependence of saturated vapour pressure of zirconium(IV) β -diketonates, *Journal of Thermal Analysis*, Vol. 46, No. 5, 1996, pp. 1367-1373.
- [14] Arul Jeevan T.S., and Nagaraja K.S., Sublimation kinetic studies of the $Zr(tmhd)_4$ complex, *Journal of Chemistry*, 2013, Article ID 350937, 5 p., <http://dx.doi.org/10.1155/2013/350937>.
- [15] Fulem M., Růžička K., Růžička V., Šimeček T, Hulicius E., and Pangrác J., Vapour pressure and heat capacities of metal organic precursors, $Y(thd)_3$ and $Zr(thd)_4$, *Journal of Crystal Growth*, Vol. 264, 2004, pp. 192-200.
- [16] Lebedev D.P., and Perelman T.L., Heat and mass transfer in the processes of sublimation in a vacuum, Moscow, Energiya, 1973, 336p. (in russ.).